Journal of Geochemical Exploration 256 (2024) 107348

Contents lists available at ScienceDirect

Journal of Geochemical Exploration

journal homepage: www.elsevier.com/locate/gexplo

New views on Somma Vesuvius subvolcanic system and on mechanism that could increase eruption explosivity by a review and immiscibility in melt inclusions

Annamaria Lima [a,*], Rosario Esposito [b]

[a] Dipartimento di Scienze della Terra dell'Ambiente e delle Risorse, Università di Napoli "Federico II", Napoli 80126, Italy
[b] Dipartimento di Scienze dell'Ambiente e della Terra, Università di Milano Bicocca, Milano 20126, Italy

ARTICLE INFO

Keywords:
Shallow magma chamber
Skarn xenolith
Silicate liquids immiscibility
Hydrosaline melt
Eruption explosivity
Magma differentiation

ABSTRACT

Somma-Vesuvius (SV) is an active volcanic system in southern Italy that has generated Plinian eruptions during its history as the infamous 79 CE (Pompeii) eruption. Plinian eruptions produced airfall pumice deposits characterized by white pumice clasts in the lower half part, and by grey pumice clasts in the other upper half part. Plinian pyroclastic deposits are also characterized by the presence of skarn xenoliths. Previous studies on the fluid (FI) and melt inclusions (MI) in the Somma-Vesuvius (SV) skarn xenoliths have widely documented immiscibility between silicate melt and hydrosaline melt (±aqueous chloride-rich liquid-carbonate/sulfate melt). In this study, we recognize a new type of MI namely composite melt inclusions (CMI) hosted in minerals of SV skarn xenoliths previously studied in the literature. In addition to a review of studies about skarn at SV, we present new microthermometric observations of CMI based on heating experiments using a heating stage. We heated CMI to complete homogenization at 1080 °C, and we cooled the CMI to simulate a natural sequence of phase appearances during magma cooling. At T around 1060 °C the CMI unmixes forming two different silicate melts. Upon further cooling at around 700 °C, the CMI show droplets of chloride immiscible liquids instantly nucleating. The cooling experiments of CMI from high-T are assumed to reproduce on a small scale the sequence of magma cooling prior to eruption below SV. In this case, magma could unmix before eruption forming two different silicate melts producing a chemically stratified reservoir. In support of our heating experiments results of CMI, the reprocessing of SV bulk rock compositions data highlights that magma feeding interplinian eruptions is Fe-and P-rich and Si-poor. In contrast, magma feeding Plinian eruptions is Si-rich and Fe-and P-poor. As experimental studies have demonstrated, immiscibility can occur when one melt is Fe-and P-rich and Si-poor, and the other is Si-rich and Fe-and P-poor and the transition between the two end members is not gradual, resulting in a gap of homogeneous intermediate melt.

1. Introduction

Understanding the dynamic processes operating in magma chambers under volcanoes is the basis for predictions of volcanic eruptions and to mitigate the risk (Geshi, 2020; Gudmundsson, 2020; Caricchi et al., 2021). The Somma-Vesuvius (SV) is a complex Quaternary volcanic system located nearby Naples (Fig. 1), in one of the most densely populated areas in Europe and for this reason it is one of the most studied volcanos of the Earth (Cannatelli, 2020 and references therein; Pappalardo and Buono, 2021). SV eruptive activity began at least 35 ka BP and the eruptive style and cyclicity have varied widely during its eruptive history; now it is in a quiescent state, with activity expressed by only fumaroles and low-magnitude seismic activity.

Fluid (FI) and melt inclusion (MI) studies effectively contributes to the knowledge of magmatic systems as they represent microscopic droplets of magma trapped in host crystal microcavity during its growing; they are closed microsystems that preserve valuable information on pre-eruptive magma composition with the volatile content that escape during the eruptions (Cannatelli et al., 2016 and references therein; Esposito, 2021, Rose-Koga et al., 2021; Wallace et al., 2021). At SV, in skarn xenoliths many FI and MI studies (e.g., Belkin and De Vivo, 1993; Lima et al., 2003) provided information on the shallow intrusive system because skarn forms along the margins of the magma reservoir. In this paper, we discuss the new perspectives on the Somma Vesuvius

* Corresponding author at: Complesso Universitario Monte Sant'Angelo, Via Cintia, 26, 80126 Napoli, Italy.
E-mail address: anlima@unina.it (A. Lima).

https://doi.org/10.1016/j.gexplo.2023.107348
Received 17 March 2023; Received in revised form 3 November 2023; Accepted 12 November 2023
Available online 16 November 2023

subvolcanic system emerging from high-T CMI cooling experiments, assuming that they reproduce on a small scale the pre-eruption magma cooling sequence, by reprocessing the SV bulk rock compositions taken from the literature and also by a previously studies review.

2. Somma Vesuvius volcanic system geological and geochemical overviews

2.1. Geology

The Campania plain in southern Italy has been related to the stretching and thinning of the continental crust by a counter-clockwise rotation of the Italian peninsula and the contemporaneous opening of the Tyrrhenian sea (Fig. 1A) at the western margin of the Apennine Chain made up by Mesozoic carbonate platforms. The regional Plio-Pleistocene fault systems by the widespread extensional tectonics, lowered by at least 3 km the carbonate platform leading the formation of the Campania Plain graben. Quaternary potassium-rich volcanism developed in central and southern Italy forming the Roman Comagmatic Province extending from Vulsini to the Vulture Volcanic Complex through Campanian plain (Pierantoni et al., 2020; Kelemework et al., 2021). SV is located on a regional Quaternary fault (Fig. 1A; Milia and Torrente, 2020). Monte Somma activity started at about 400 ka (Brocchini et al., 2001; Di Renzo et al., 2007), Somma caldera formed by Plinian eruptions (between 25 and 8 Ka) that destroyed the volcanic edifice and led to the collapse of the eruptive vent (Rolandi et al., 2004).

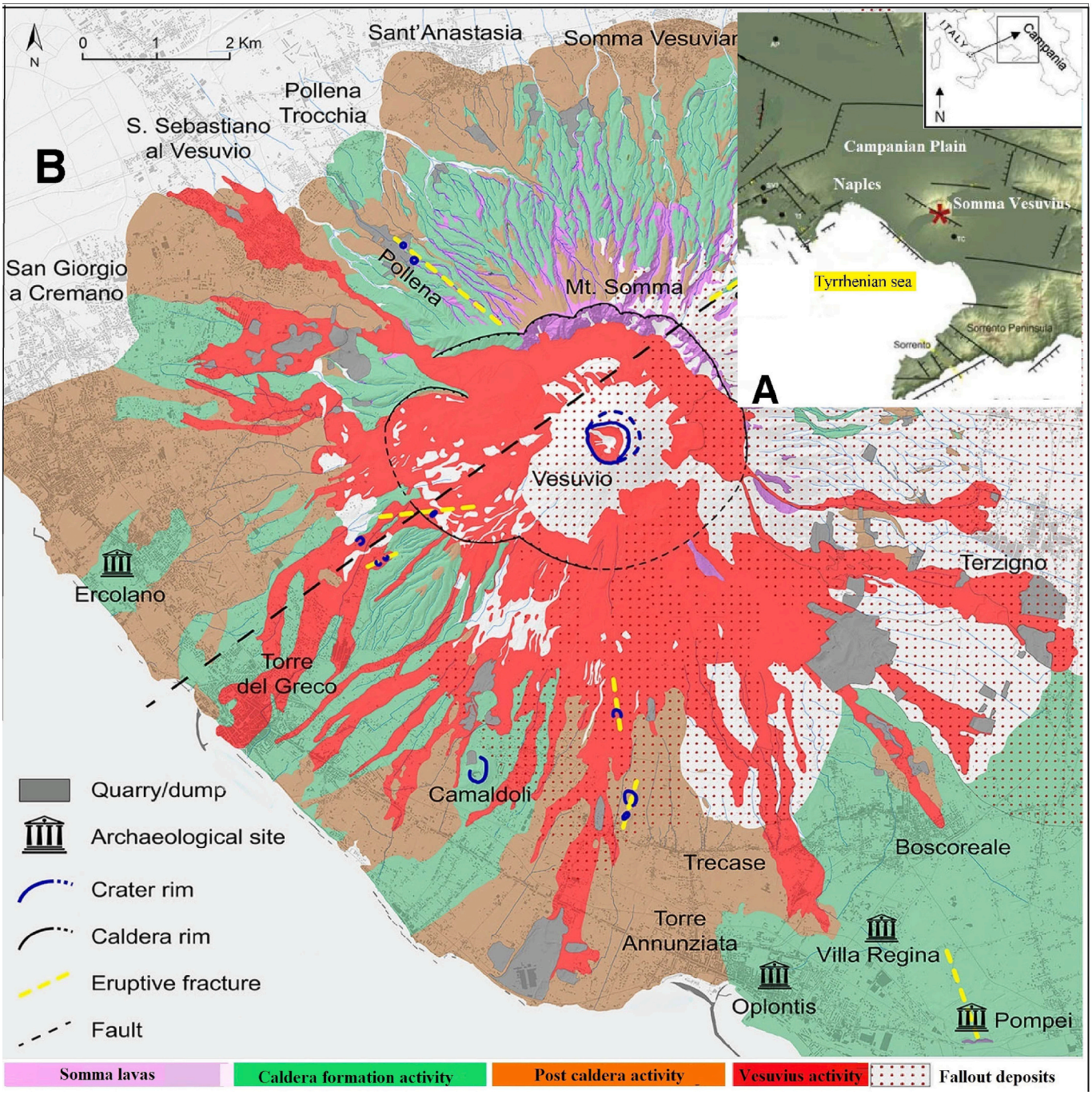

Fig. 1. Structural map of the Campanian Plain modified after Milia and Torrente (2020) (A), and (B) geological map of Somma Vesuvius system modified after Sbrana et al. (2020).

Vesuvius is a stratovolcano formed within the Somma caldera after the 472 CE Plinian eruption (Fig. 1B; Rolandi et al., 1998, 2004; Linde et al., 2017).

Much information on SV basement lithology were obtained in 1980 by the Trecase well (Fig. 2B). It is about 1900 m deep, located on the southern slope of Vesuvius at about 3 km far and the temperature measured at the bottom of the well was of 50 °C. After a sedimentary sequence of siliciclastic and volcanic rocks 1880 m thick, limestone rocks were encountered (Bernasconi et al., 1981). SV volcanic system is located within a sequence of about 6 km thick of Meso-Cenozoic limestones and dolostones overlayed by Miocene age sediments (Zollo et al., 1998; Milia et al., 2003; Milia and Torrente, 2020; Nunziata et al., 2020; Pierantoni et al., 2020). The SV plumbing system is interpreted to be a complex feeding column (Fig. 2B) that is dominated by multiple mush zone and thus includes a variety of local crystallization environments characterized by contrasting cooling rates and P–T conditions (Fig. 2A). The shallowest reservoir is at a depth corresponding to a pressure of about 100 MPa (Fig. 2C). Geobarometric studies (Fig. 2A) by FI in xenoliths and cognate nodules erupted by SV documented the presence of several magma chambers/reservoirs ranging from 3.5 to 10 km and a large one at depth > 12 km (Belkin et al., 1985, 1998; Belkin and De Vivo, 1993; Klébesz et al., 2012, 2015) (Fig. 2A, B and C). These depths have been confirmed by seismic, tomographic, aeromagnetic, and gravimetric studies (Berrino et al., 1998; Fedi et al., 1998; Auger et al., 2001; Zollo et al., 1996, 1998; De Natale et al., 2003, 2006) and by magnetotelluric evidence (Di Maio et al., 1998). Fig. 2C also shows the types of inclusions found in skarn xenolith samples which provided important information on the SV subvolcanic system (Gilg et al., 2001; Fulignati et al., 2001).

SV volcanic activity (Fig. 3) has been divided into three megacycles (composed of several smaller cycles) based on the systematic major and trace element variations in whole rock chemistry during time (Ayuso et al., 1998). Each magmatic megacycle starts always with a Plinian eruption and ends by a long repose time. The first megacycle (purple in Fig. 3) includes the activity between 25 and 14 ka, corresponding to the formation of Monte Somma; the second megacycle (green in Fig. 3) between 8 and 2.7 ka includes, among others, Ottaviano (about 8 ka) and Avellino (about 3.5 ka) Plinian eruptions. The third megacycle (pink in Fig. 3), the most recent, between 79 and 1944 CE, includes Pompeii (79 CE) and Pollena (472 CE) Plinian eruptions and the 1631 CE

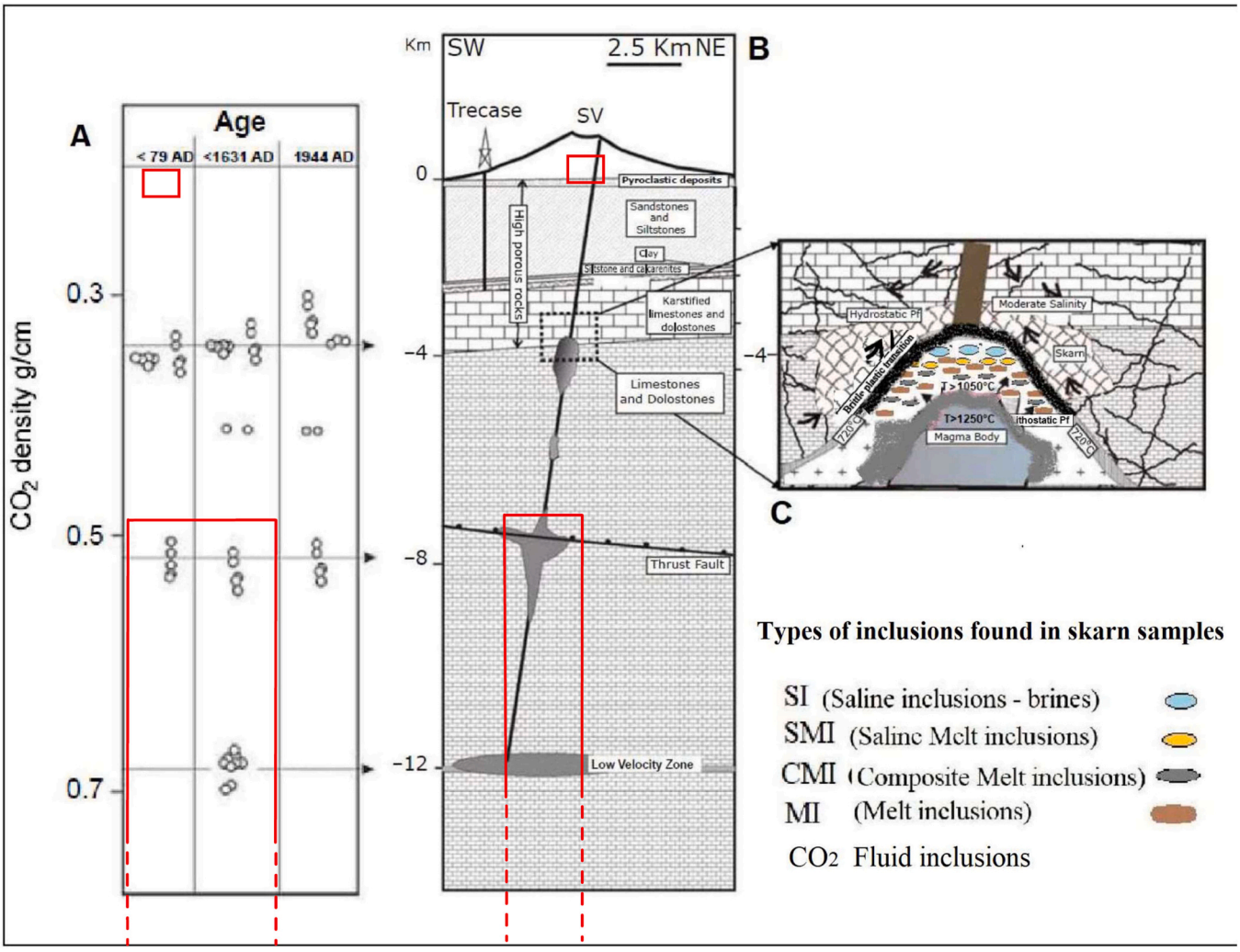

Fig. 2. A) CO_2 density by FI trapped in olivine and pyroxene crystals of the SV cognate nodules utilized to infer magma chamber depths (Belkin et al., 1985). B) Stratigraphic succession below SV (Milia et al., 2003) and depth of magmatic chambers as by Lima et al. (2007). Trecase well location is also shown (see text). C) SV shallow magma chamber, at close conduit condition, with the "transition zone" between magma-dominated system and fluid-dominated system where skarn rocks form (Lima et al., 2007). Trapped different inclusion types in growing crystals as described in the literature are also shown (Gilg et al., 2001; Fulignati et al., 2001). Red boxes indicate depths of formation of reheated MI hosted in olivines of Somma interplinian lava flows, Avellino, Pompeii-79 CE, Pollena-472 CE, and 1631 CE eruptions reported by Esposito et al. (2023). (For interpretation of the references to colour in this figure legend, the reader is referred to the web version of this article.)

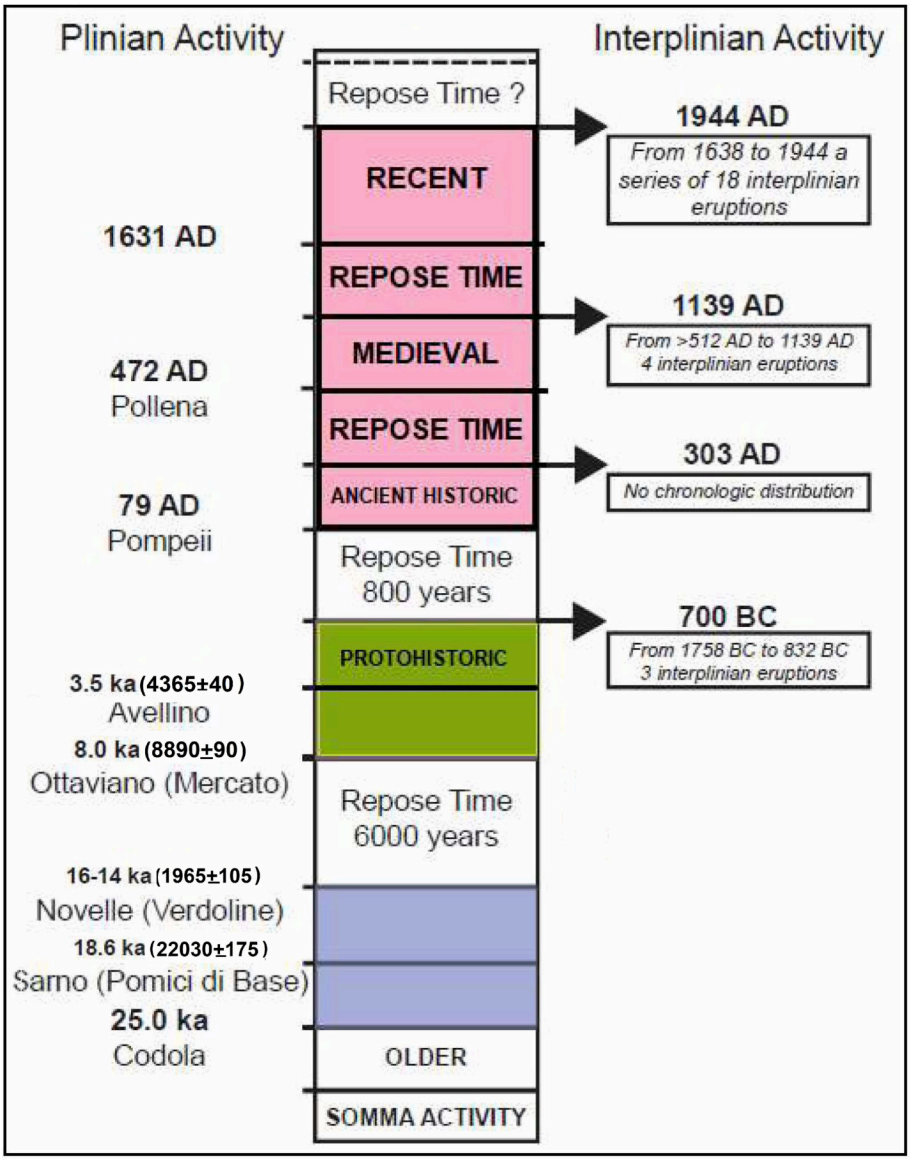

Fig. 3. History of Somma Vesuvius Plinian and interplinian volcanic activity grouped into three megacycles based on Ayuso et al. (1998). The activity of the megacycle III is colored in pink, the activity of megacycle II is in green, and the activity of megacycle I is in purple. Nomenclature of eruptive events is as by Rolandi et al. (1998 and 2004). Nomenclature in parentheses is as by Santacroce (1987). The age of the eruptions and the repose time are based on Rolandi et al. (1998). Ages in years before the present in parentheses are calibrated as reported by Santacroce et al. (2008). (For interpretation of the references to colour in this figure legend, the reader is referred to the web version of this article.)

subplinian one. The 79 CE Plinian eruption took place after a repose time of 800 years, Pollena after 169 years of repose time and the 1631 sub Plinian one after 492 years of repose time. Each Plinian or subplinian event is followed by weak to moderately explosive or explosive-effusive interplinian activity (Fig. 3) with the emplacement of scoria and lava flow (Rolandi et al., 1998).

The pumice deposits of SV Plinian eruptions show geochemical gradients that have been interpreted to reflect the progressive withdrawal of the shallow magma chamber chemically (and density) stratified (Civetta et al., 1991; Civetta and Santacroce, 1992; Rolandi et al., 1993; Cioni et al., 1995; Landi et al., 1999; Santacroce et al., 2008; Melluso et al., 2022). To explain the pre-eruptive stratification several processes have been hypothesized such as crystal-liquid fractionation by simple chemical differentiation of unique parental magma (Landi et al., 1999; Buono et al., 2020), by the arrival of diverse magma batches from deeper reservoirs (e.g., Civetta et al., 1991; Cioni, 2000) and by magma withdrawal dynamics (Sigurdsson et al., 1990). This topic is still debated. In the last 79 years the SV system seems to be in a repose time.

2.2. Geochemistry

SV volcanic products consist of potassium-rich rocks that show a large compositional variation in alkali contents with variable K_2O and silica (Fig. 4; Peccerillo, 2003, 2020, Melluso et al., 2022). The compositions of Plinian and subplinian volcanic rocks are usually more evolved (MgO < 4 wt%) than the interplinian ones (Fig. 5B) whose composition remained unchanged since the 79 CE eruption (Fig. 5; Lima et al., 2003; Santacroce et al., 2008). The degree of silica undersaturation increases with time and SiO_2 content is the lowest in the third megacycle volcanic rocks (Fig. 5). The megacycles are not characterized by distinct isotopic ranges because the three groups show overlapping compositions with a large variability within each cycle (e.g., Ayuso et al., 1998; Piochi et al., 2006). The Sr-isotope compositions found in SV stratigraphic sequences of different eruptions show a trend

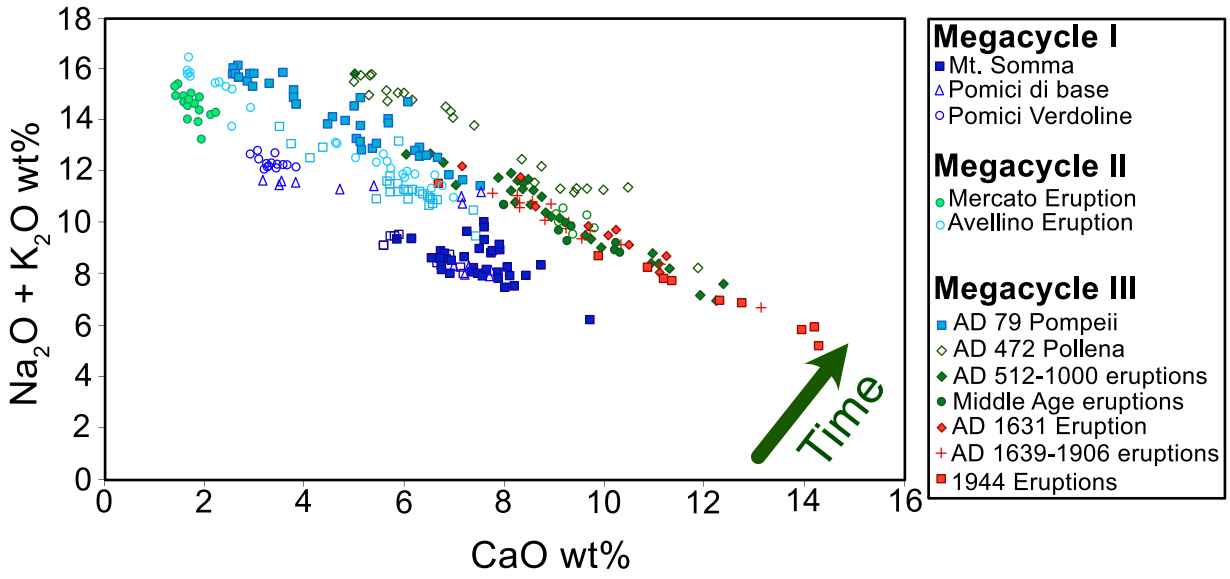

Fig. 4. Total alkali versus CaO concentrations of bulk rocks of SV modified after Sbrana et al. (2020). Bulk rocks data are by Santacroce et al. (2008).

interpreted as the arrival of Sr-isotopically different magma batches (Di Renzo et al., 2022). Plinian and subplinian eruptions give rise to pumice sequences formed by white pumice at the bottom and grey pumice at the top. They show a marked vertical compositional variation, and the white pumices are enriched in Na_2O (Fig. 6). The Pompei pumice deposits, studied in detail (e.g., Civetta et al., 1991; Sigurdsson et al., 1990) show a sharp upward transition from white phonolite pumices with more sialic compositions at bottom of the deposits and the less evolved tephritic grey pumices on the top in addition, a compositional gap separating white from grey pumices (Fig. 6A).

Grey and white pumices have distinct Sr and Nd isotopic compositions. Whole rocks δO^{18} values range from about 7.5 ‰ to about 10 ‰ (Fig. 7A) and there are no correlations with Nd, Pb and Sr isotopic compositions. Additionally, δO^{18} shows a positive correlation with the degree of chemical evolution with time (Fig. 7A; Piochi et al., 2006). Lava and scoria δO^{18} values are lower than the δO^{18} of pumices (Fig. 7A); the latters have δO^{18} approximately 1.4 ‰ higher than the lavas. These differences show that, at least, at the scale of each group, there is isotopic zoning (Ayuso et al., 1998).

Closed system fractional crystallization was not the controlling process that produced the observed isotopic variations (Fig. 7C; Ayuso et al., 1998). In addition, the δO^{18} variation at nearly constant silica content in pumices from Plinian eruptions from the 3rd megacycle has been interpreted to be the result of O isotope exchange, mediated by a volatile-rich aqueous fluids between the upper parts of the magma chamber and the surrounding carbonate country rock (Ayuso et al., 1998). White and grey pumices have different Sr isotope compositions as well. Both pumice types contain feldspars with a constant Sr isotopic composition, like that of white pumices, interpreted as Sr isotopic disequilibrium in rocks upwards in the sequence and mingling of magmas during eruption (Civetta et al., 1991). Moreover, the lowermost part of the 79 CE eruption and the uppermost part of Avellino have similar $^{87}Sr/^{86}Sr$ values (Fig. 7B), suggesting that magma remnants can be left behind within the chamber after large magnitude events (Civetta et al., 1991; Civetta and Santacroce, 1992; Piochi et al., 2006). The incomplete magma removal has also been suggested by evidence that events following Plinian or sub Plinian eruptions produced magmas that have isotopic characteristics comparable to those of previous eruptions (Civetta and Santacroce, 1992; Piochi et al., 2006) (Fig. 7B).

3. Previously studied fluid and melt inclusions in skarn minerals

In SV volcanic products, including surges and flows from mostly Plinian and subplinian explosive eruptions many types of xenoliths have been found. They provided information on SV magmatic system. Xenoliths show wide variability in composition and texture and have been divided into ultramafic cumulates, skarns, hornfels, and syenitic subvolcanic rocks (Hermes and Cornell, 1978, 1981, 1983).

Skarns have been interpreted by some as rocks formed by metasomatic processes, i.e., solid state reactions through the interaction of fluids (e.g., Turner, 1981). At SV, MI studies indicate that skarns crystallized from a magmatic melt at depths equivalent to 66 and 137 MPa (about 2.5–5 km deep, assuming a rock density of 2.7 g/cm^3). These depths were calculated by both primary CO_2 FI (Fig. 2A) and aqueous FI salinity in skarn minerals (Hermes and Cornell, 1978, 1981, 1983; Belkin et al., 1985; Belkin and De Vivo, 1993; Gilg et al., 2001; Fulignati et al., 2001, 2005; De Vivo et al., 2006; Lima et al., 2003, 2007).

Studied skarn xenoliths (Fulignati et al., 2001; Gilg et al., 2001; Lima et al., 2007) are representative of the SV shallow intrusive system, along the top and sides of the magma reservoir. Here a transition zone forms between a magma dominated system and a fluid dominated system and various inclusion types have been trapped in growing crystals (Fig. 2C). They have been classified by their appearance at room temperature as:

- CO_2 FI: CO_2-rich inclusions, mostly vapor-rich. They appear to contain either a single phase or liquid + vapor. They are generally with a roundish shape and can be both primary and secondary. CO_2 has been trapped often along with silicate glass and H_2S (Fig. 8A).
- Saline inclusions (SI type) may display subspherical, negative crystal or irregular shapes. They contain two or more isotropic soluble daughter minerals and a visible aqueous phase. The vapor bubble may contain CO_2 and sometimes H_2S (Fig. 8B).
- Multiphase hydrosaline-melt inclusions also called saline-melt inclusions (SMI type) appear completely crystallized; vapor bubble is difficult to recognize. SMI show commonly other birefringent and/or opaque minerals (Fig. 8D–F and inclusions a and b in Fig. 10).
- Melt inclusions (MI type) appear brown, in different shades, as silicate glass (melt) with one or more bubbles. Other MI show dark globules inside of different sizes and irregular shapes (Fig. 8C).

The SMI show the immiscibility between silicate melt and hydrosaline-melt, also called salt melt (± aqueous chloride-rich

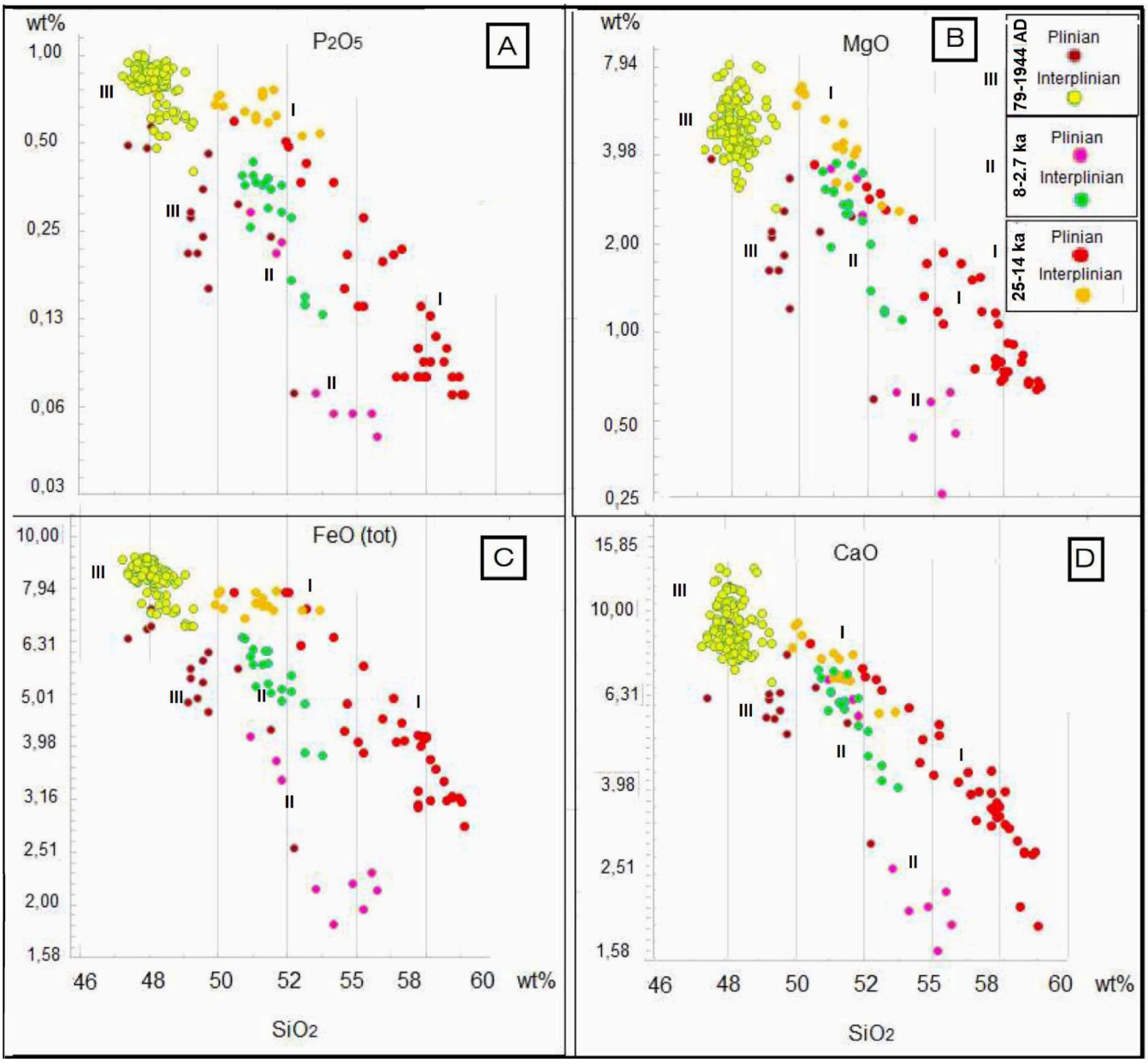

Fig. 5. Bulk rock P_2O_5, MgO, FeO (total) and CaO versus SiO_2 (data from Ayuso et al., 1998). Plots have been performed by logarithmic transformed data to produce the smallest error possible when making a prediction. Antilogarithmic values have been reported on the graphs.

liquid-carbonate/sulfate melt). There are several studies reporting the formation of immiscible liquids during the microthermometric experiments of inclusions at SV (De Vivo et al., 1995; Gilg et al., 2001; Fulignati et al., 2001, 2005; Kamenetsky, 2006; Kamenetsky et al., 2003). In SV skarn SMI occur in wollastonite, gehlenite, scapolite and fassaitic clinopyroxene. During microthermometric experiments on heating and on cooling (Gilg et al., 2001; Fulignati et al., 2001) SMI show the formation of hydrosaline-melt globules (Fig. 9A and B). The latters separating from the melt converge in a pocket of liquid that binds to the vapor bubble (Fig. 9A1 and B2). During heating the liquid hydrosaline-melt globules form and join in the pocket which grows and then with further increase in T it shrink gradually until complete homogenization at around 870 °C occurs (Fig. 9A2) conversely, on cooling the unmixing is instantaneous at a temperature < 700 °C.

4. New inclusions in skarn minerals named composite melt inclusions (CMI)

4.1. Analytical methods

For this study we performed 18 heating experiments of CMI hosted in wollastonite and in gehlenite from SV skarn xenoliths. For the heating experiments we have employed the Linkam TS1400XY heating stage (Esposito et al., 2012). We have used a N gas flow (0.5 ± 5 % liter/min) during experiments. We have used ca. 50 μm gold flakes as standards to calibrate the instrument at the melting point of gold (1064 °C) using heating ramps as 100 °C/min from 25 to 900 °C, 50 °C/min from 900 to 1000 °C, and 25 °C/min from 1000 to 1100 °C (Esposito et al., 2012). Based on this calibration the error for the T during experiments is ca. 5 °C. The CMI was heated up to 1100 °C, and cooled to room temperature at a rate of 20 °C/min.

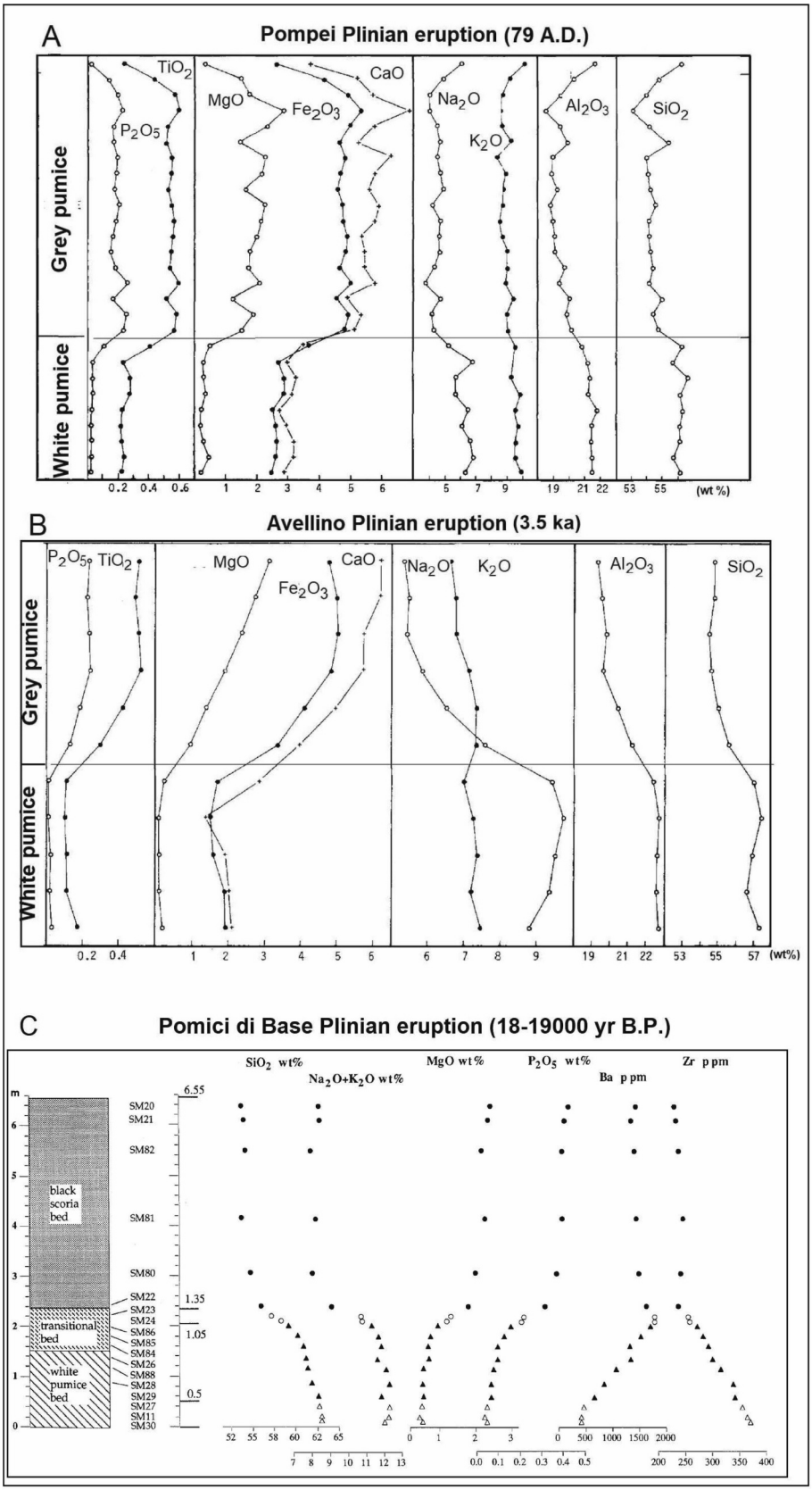

Fig. 6. Vertical chemical variations of pumices of A) Pompei eruption and B) Avellino eruption Analyses are in wt%, water-free and recalculated to 100 %; Fe_2O_3 is the total Fe (after Civetta et al., 1991 modified); C) Pomici di Base chemical variations along the Plinian fall sequence (after Landi et al., 1999, modified).

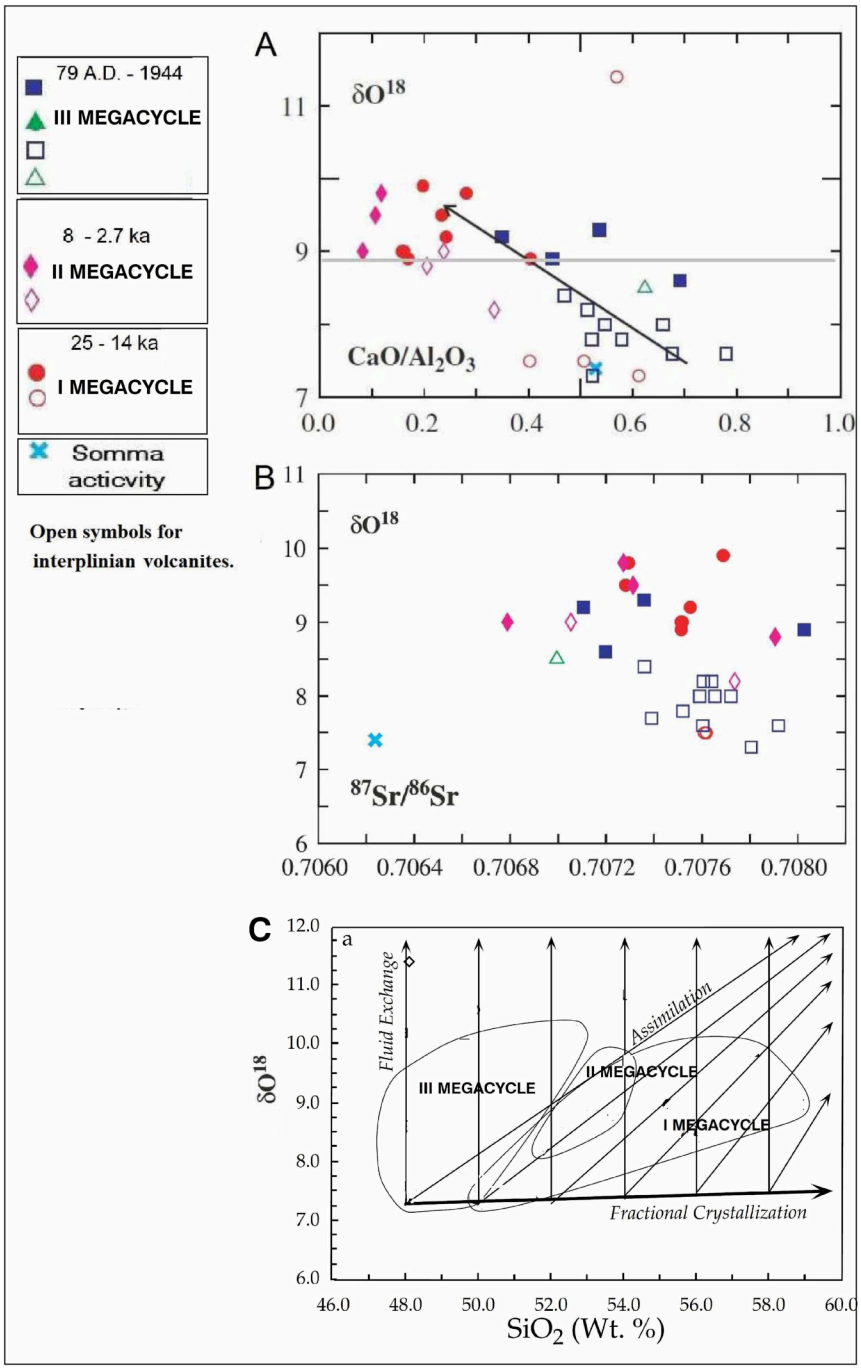

Fig. 7. A) δ O^{18} (‰) versus CaO/Al_2O_3. B) δ O^{18} (‰) versus $^{87}Sr/^{86}Sr$. The full symbols refer to the Plinian volcanics, the open symbols to the interplinian ones (from Piochi et al., 2006, modified). C) δ O^{18} (‰) versus SiO_2 plot showing pumices, lavas and scorias from each megacycle; vectors illustrating fluid phase exchange, assimilation, and fractional crystallization processes (from Ayuso et al., 1998 modified).

4.2. Composite melt inclusions (CMI)

Composite melt inclusions (CMI) have been found for the first time (Fig. 10c) in already studied SV skarn xenoliths along with SMI and CO_2 FI (Fig. 10a, b and d) reported in previous studies (De Vivo et al., 1995; Gilg et al., 2001; Fulignati et al., 2001, 2005; Kamenetsky, 2006; Kamenetsky et al., 2003). CO_2 FI indicate a formation depth of about 100 MPa, as reported in previous studies on the same samples (e.g., Gilg et al., 2001). Fig. 10 shows SMI, CMI and CO_2 FI found in the same wollastonite crystal. They have a close genetic relationship because they coexist within the crystal growth planes (Fig. 10) and because during experiments show the same behavior at least until about 700 °C. The great difference is that CMI record the complete sequence of all the phases of magma cooling.

At room temperature it is very difficult to distinguish CMI from SMI (Fig. 10). Like SMI they occur in wollastonite, gehlenite, scapolite and clinopyroxene and only the small size inclusions (about 20 μm) do not decrepitate during heating/cooling experiments (Figs. 11 and 12). After the complete homogenization of the CMI (at T > 1060 °C), on cooling experiment, at about 1060 °C, two different immiscible liquid phases form interpreted silicate melts. Fig. 12 and the supplementary video show one of the clearest cooling experiments of a CMI previously heated up to 1080 °C (Fig. 12a). On cooling (20 °C/min) at about 1060 °C two liquid pockets formed (Fig. 10b–d), interpreted as two immiscible

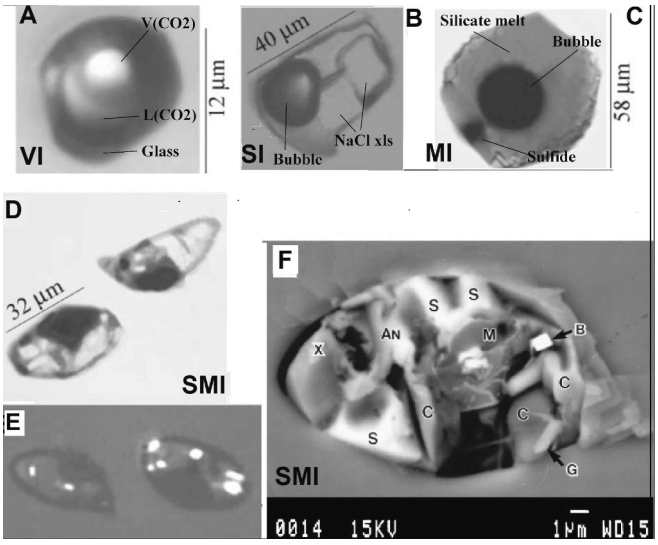

Fig. 8. Types of inclusions found in skarn minerals. A) Primary CO_2 inclusion vapor-rich (VI) in wollastonite at room temperature. It contains vapor CO_2, liquid CO_2 and silicate glass. B) Hydrosaline inclusion (SI) in wollastonite with two isotropic cubes of NaCl. C) Magmatic inclusion (MI) in wollastonite with shrinkage bubble and sulfide globule. D, E and F) Multiphase hydrosaline-melt inclusions (SMI) in gehlenite; E) the same SMI as in D with crossed polarizers to show the birefringent minerals; F) SEM image of an open SMI (similar to D); the phases identified are: sylvite (S), barite (B), calcite (C), a hexagonal crystal of biotite mica (M) and anhydrite (An). Other identified phases are K, Na sulfate (X) perhaps aphthitalite, Na, Ca sulfate (G), possibly glauberite (from Gilg et al., 2001).

silicate melts due to the high homogenization temperature. Cooling on, at about 700 °C an instantaneous unmixing (Fig. 10e), like the one observed in SMI (Fig. 9) occur between hydrosaline melt and silicate melt. The supplementary video at about 700 °C shows a quick flash when unmixing takes place instantly. In this video an experiment lasting 4/5 h was synthesized in <2 min. The right shot took place after 18 experiments which gave unclear images.

4.3. CMI formation in SV subvolcanic system

According to the model shown in Fig. 2 (Lima et al., 1999, 2003, 2007), in the shallow magma chamber, located approximately at a depth equivalent to 100 MPa (Belkin et al., 1985; Belkin and De Vivo, 1993), within the carbonate country rock, during repose time (Fig. 3), before a Plinian eruption, the magma resides for long time in a closed conduit condition and very saline fluids (brine) and gases by magma vesiculation (second boiling) cannot escape (see also Bodnar et al., 2007; Lima et al., 2021). In the "transition zone" between the magma-dominated system and fluid-dominated system, H_2O reacts with the chloride, fluoride, borate, and carbonate species. The chemical effects of high temperature hydrolysis may be enhanced by phase separation and multiple immiscible fluid phases can form (Veksler and Charlier, 2015); limestone and dolomitic country rocks melt, as a result of infiltrative contact metasomatism associated with silicate magmas (Lentz, 1999, 2017), increasing both $P(CO_2)$ and Ca and Mg content in the melts. The modified silicate magma separates into co-existing immiscible melts with different viscosities that by dynamic interaction would partition elements, as well as isotopic signatures (Lentz, 2017). On the other hand, O isotopic compositions (Fig. 7), for SV pumice, lava and scorias for each group, indicate crustal assimilation and fluids exchange processes (Ayuso et al., 1998; Piochi et al., 2006). In the last decade most researchers argued for the involvement of carbonate melts at SV volcanic system using mostly isotopic evidence. Ayuso et al. (1998) based on the geochemical and isotopic (Nd-Pb-Sr-O) variations on a suite of 150 samples of SV volcanic rocks, suggested an isotopic exchange between magma and limestone, near the roof of the magma chamber; Gilg et al. (2001), studying C and O isotope compositions of skarn, calcites and silicate melt inclusion-bearing wollastonite nodules, suggested assimilation of carbonate wall rocks by the alkaline magma at moderate depths (<5 km). The interaction between early high-temperature hypersaline fluids, carbonate country rocks and residing magma for long periods of time is best recorded in all inclusions trapped in skarn minerals (Fig. 2C; De Vivo et al., 1995; Gilg et al., 2001; Fulignati et al., 2001, 2005; Kamenetsky, 2006; Kamenetsky et al., 2003). CMI record on a micrometer scale the complete sequence of all magma cooling phases, which most likely also occur on a large scale at the SV.

5. Discussion

In this review, various aspects of the SV volcanic system have been highlighted that have not yet been clarified despite the large number of studies carried out so far. The results of previous studies on FI and MI in SV skarn minerals have been reported, together with new preliminary microthermometric observation on CMI.

Until now immiscibility, between silicate melt and hydrosaline melt (±aqueous chloride-rich liquid-carbonate/sulfate melt) have been widely documented at SV and in other subvolcanic Italian systems as well. Good examples are at Campi Flegrei (De Vivo et al., 2006; Fedele et al., 2006; Bodnar et al., 2007; Lima et al., 2009), at islands of Ponza (Belkin et al., 1996; De Vivo et al., 2006) and Ventotene (De Vivo et al., 1995; Fulignati et al., 2005) and at Pantelleria in the Sicily Channel (De Vivo et al., 1992, 1993, 2006; Lowenstern, 1993, 1994).

A new finding is the immiscibility between silicate liquids, with different chemical compositions which could explain the observed stratification in SV magma chamber.

5.1. Silicate liquids immiscibility

Silicate liquids immiscibility (SLI) is one of the differentiation processes in magmatic systems. Experimental studies (e.g., Roedder, 1979; Philpotts, 1979, 1982) have demonstrated that it can occur in two type of silicate melts: 1) in highly Fe-rich basaltic melt, where one liquid is Fe-and P-rich and Si-poor, and the other is Si-rich and Fe-and P-poor; 2) in highly alkaline melts. In an extensive review of the petrogenetic significance of SLI, Roedder (1979) was able to list 40 references proposing immiscibility in various natural rock bodies. Evidence for SLI can be found in many tholeiitic basalts where minute globules of dark brown glass are set in a matrix of paler glass (Philpotts, 1979; Belkin et al., 2009). Another demonstration of SLI occurs between high Fe basaltic melts and highly alkaline melts (Veksler, 2004; Veksler et al., 2007; Lino et al., 2023). Occurrence of SLI during cooling of magmas have been shown in layered intrusions as well (i.e., the Skaergaard; Holness et al., 2017). Currently, it is broadly accepted that SLI occurs at the late stage of magma evolution following large magma differentiation by fractional crystallization, mostly at marginal zones of magma chamber (e.g., Veksler and Charlier, 2015). The SLI can become increasingly important at near-solidus temperatures, so that, the solidus itself is difficult to define. The SLI is difficult to recognize at large scale mostly because it can show petrologic signatures like magma mixing and/or mingling. Once two or more fluids separated, they behave exactly like different magmas with different composition and mobility. However, an implication of SLI is that compositions between unmixed pairs cannot exist as homogeneous melt and this give rise to a gap of intermediate homogeneous melts during magma cooling and differentiation (Lino et al., 2023). In previous studies, even if SLI in not invoked, trapping in the same crystal of MI with different compositions has been reported. Belkin et al. (1985), studying FI in SV xenoliths, pointed out that in skarn samples there are two types of MI with a different behavior during heating/cooling experiments and speculated that they trapped melt of different composition. Lima et al. (2006 and 2007) found that MI in

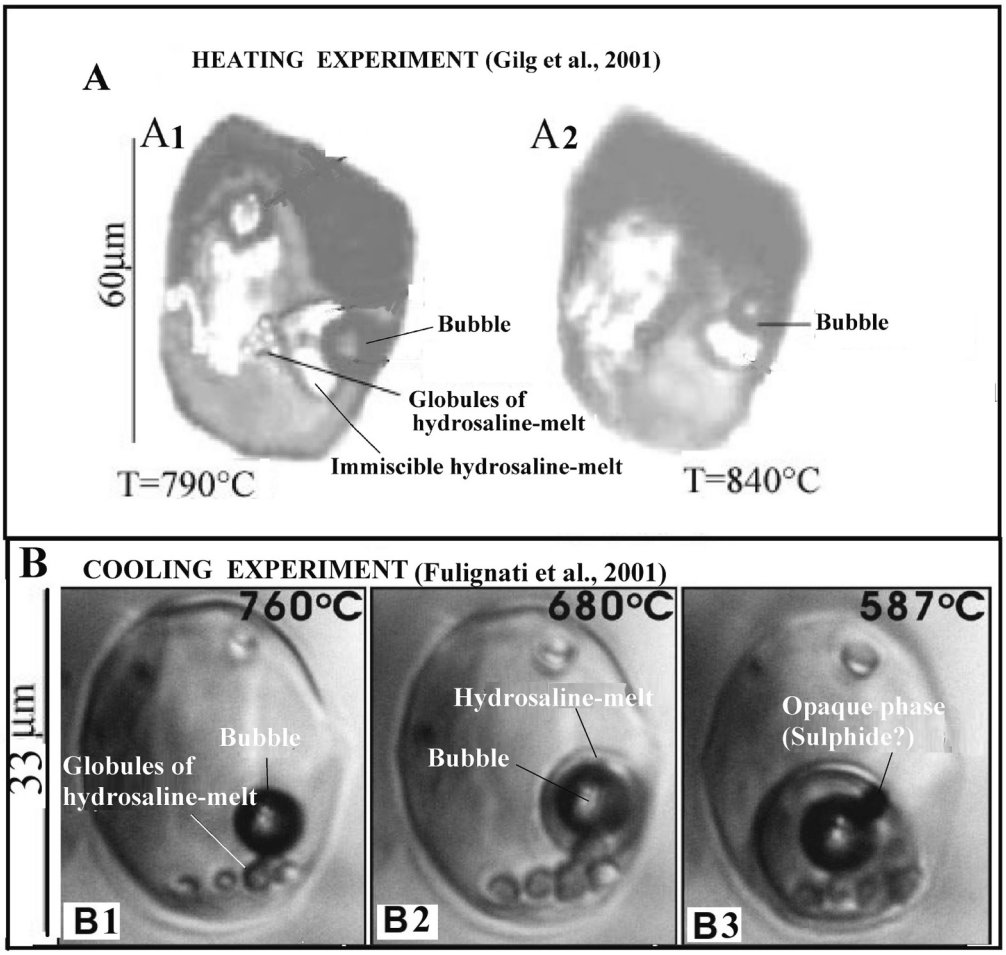

Fig. 9. A) Heating experiment of a multiphase hydrosaline-melt inclusion (SMI) in gehlenite from SV skarn (for the composition at room T refer to Fig. 8F). A1) On heating hydrosaline-melt globules form and join in a liquid pocket that binds to the vapor bubble. A2) With further increase in T the immiscible liquid pocket shrinks gradually until complete homogenization at about 870 °C occurs (Gilg et al., 2001). B) Cooling experiment of a multiphase inclusion (in nepheline or clinopyroxene) from the SV skarn xenolith (the same type of SMI in Fig. 8F). B1 and B2: On cooling hydrosaline-melt globules form and join in a liquid pocket that binds to the vapor bubble, unmixing between two liquids at temperatures <680 °C occurs; B3) opaque phase (sulfide?) forms at 587 °C inside hydrosaline- melt (Fulignati et al., 2001).

clinopyroxenes and olivines from SV 79 CE pumice samples show compositions representing two different populations in the same crystal.

The Pomici di Base-Sarno Plinian eruption, the largest eruptive SV event (Bertagnini et al., 1998; Buono et al., 2020), produced 6.5 m of compositionally zoned trachyte to latite fallout deposits. Klébesz et al. (2012, 2015) studying this eruption, report that in the same clinopyroxene crystal two different types of MI with different compositions, spatially associated and very likely genetically related. Sigurdsson et al. (1990) found that the composition of glassy MI, in pumice phenocrysts of the Plinian eruption of 79 CE, indicates that prior to the eruption in the magma chamber, there were two dominant magma types and there was no continuous compositional gradient. They also estimate that the H_2O content for Plinian magma that give rise to white pumices was 4.7 and for the grey pumice 3.5 ± 0.50 wt% based on analysis of glasses of MI using the total difference method.

5.2. SV stratified magma chamber by silicate liquid immiscibility

As discussed in the previous paragraph, at a large scale, SLI can show petrologic signatures like magma mixing and/or mingling and for this reason all the previous data supporting this hypothesis should be considered. If CMI accurately reproduces on a small scale the sequence of phase separation events in the shallow magma chamber, this suggests that the magma on cooling at T < 1060 °C, unmixes forming two different silicate melts independently evolving to different degrees and over time becoming stratified. Once two or more melts form, they behave as different magmas, with petrological signatures which can be misinterpreted as magma mixing and/or mingling. As experimental studies have demonstrated, immiscibility can occur when one melt is Fe- and P-rich and Si-poor, and the other is Si-rich and Fe-and P-poor (Roedder, 1979; Philpotts, 1979, 1982) with the lack of intermediate homogeneous melt.

Fig. 5 shows the plots made by logarithmic transformed data utilizing the SV database containing the bulk rock geochemical analysis of 150 pumice, scoria and lava samples (De Vivo et al., 2003) grouped according to the three megacycles (Fig. 3). For all three megacycles magma feeding interplinian eruptions are rich in Fe-, Ti-, P- Mg- and Ca and poor in Si compared to the Plinian ones (Fig. 5). In addition, the more recent third megacycle, starting with the Plinian eruption of Pompei, and the second megacycle, that begins after the formation of the Somma caldera, show two clusters and the lack of intermediate compositions (Fig. 5). Likely, after the caldera formation, during the long repose time, the steady-state magma differentiated by SLI forming two layers (Fig. 5). Below the magma that feeds the interplinian eruptions and above the less dense magma that feeds the Plinian eruptions. The latter cools down slowly, at about 1060 °C differentiates by SLI forming in turn two layers (Fig. 6). The denser one at bottom will give rise to grey pumices and the top one will give rise to white pumices, assuming the upper layer erupted first. Magma feeding white pumices, on the top layer, resides in the "transition zone" and it undergoes significant

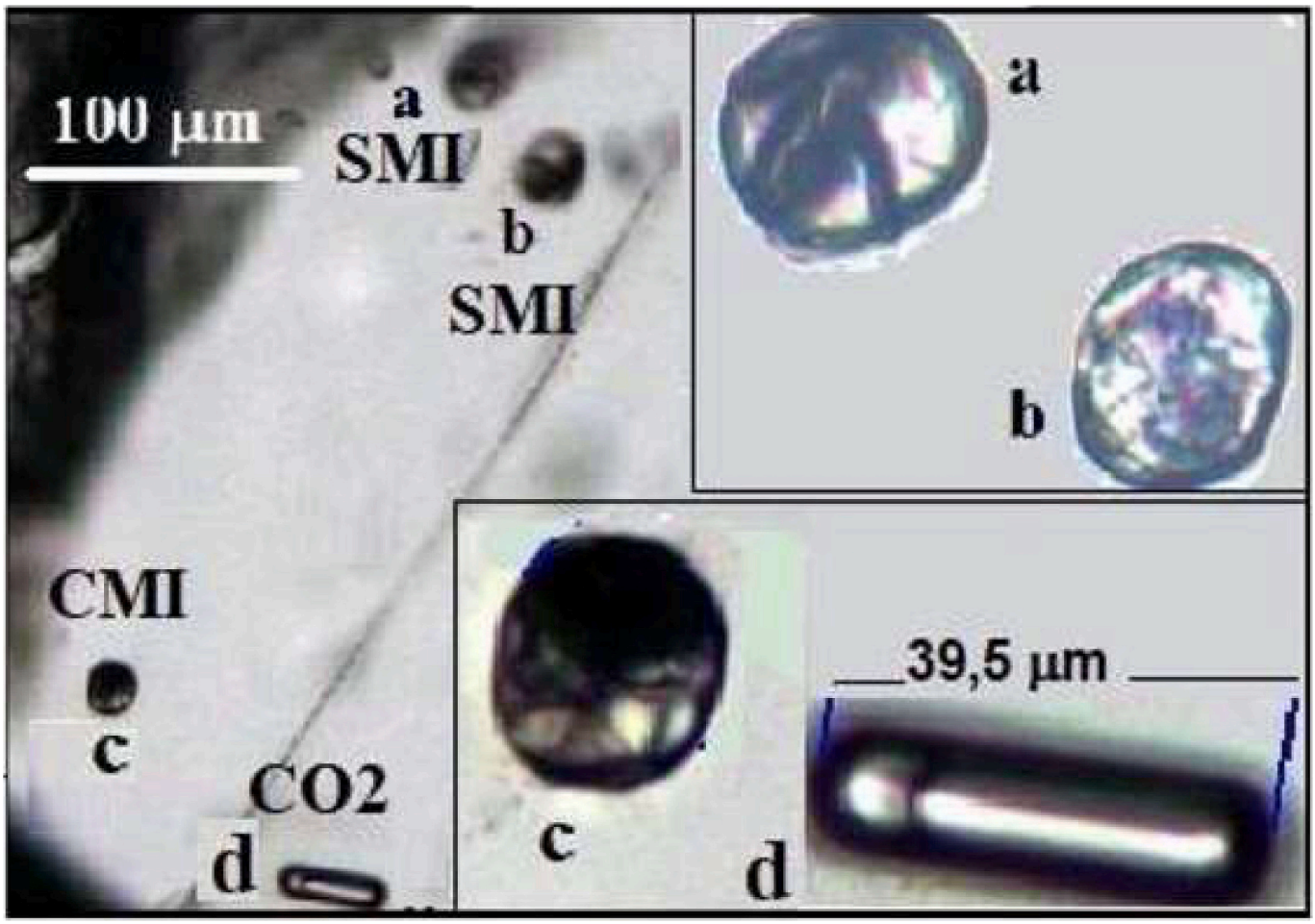

Fig. 10. A skarn wollastonite crystal trapped different type of inclusions, at room temperature (RT): a,b = multiphase hydrosaline-melt inclusions (SMI), for composition at RT refer Fig. 8F; c = composite melt inclusion (CMI), see text, and d = CO_2 fluid inclusion vapor rich, for RT phases refer Fig. 8A.

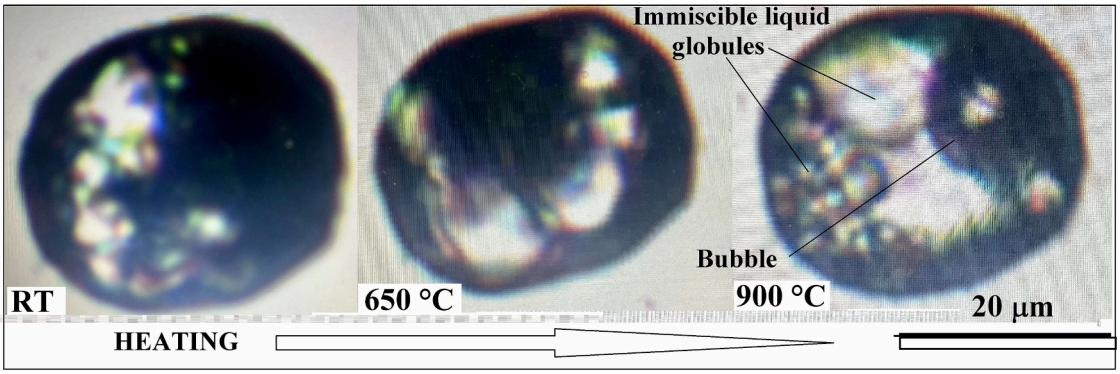

Fig. 11. Composite melt inclusion (CMI) in wollastonite crystal, the same shown in Fig. 10c and in Fig. 12, during heating experiment at Naples Fluid Inclusion Lab, at different temperatures. The composition of the immiscible liquids (L1 and L2) that form is unknown.

geochemical changes, as do the isotopic signatures and H_2O content of melt. For the latter, Sigurdsson et al. (1990) studied the 79 CE Pompei eruption and reported that MIs hosted in phenocrysts of white pumice deposit showed H_2O concentration up to 4.7 wt%, while the MI hosted in phenocrysts of grey pumice deposit showed lower H_2O content about 3.5 wt%.

Magma feeding interplinian eruptions would remain at the bottom of the shallow magma chamber until the upper layers are exhausted by Plinian eruptions. This could also explain why interplinian erupted magmas show little variations in the composition and resemble the result of a steady state under the volcano (Fig. 5; Civetta and Santacroce, 1992; Lima et al., 2003; Lima et al., 2006; Santacroce et al., 2008). A new repose time could begin when the deeper interplinian magma layer is empty. Chemical zonation of pumice deposits of Plinian eruptions, characterized by an abrupt rather than gradual compositional change (Fig. 6) and isotopic data, corroborate the SLI role on the shallow magma chamber stratifications.

As observed during heating/cooling experiments (Fig. 12 and the supplementary video), immiscibility between silicate melt and hydrosaline melt instantaneously occurs at about 700 °C. Unmixed droplets of

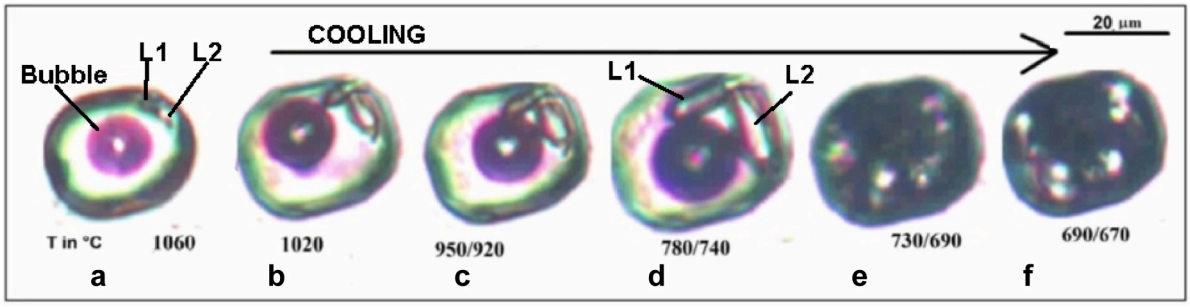

Fig. 12. CMI during cooling experiment, at Naples Fluid Inclusion Lab (see also the supplementary video); a) inclusion is not completely homogenized to avoid decrepitation; b) two melt pockets start to grow separately; c and d) melt pockets increase in volume; e) at about 700 °C in a flash there is a rapid formation of immiscible fluids; f) droplets converge in the different formed pockets/bubbles.

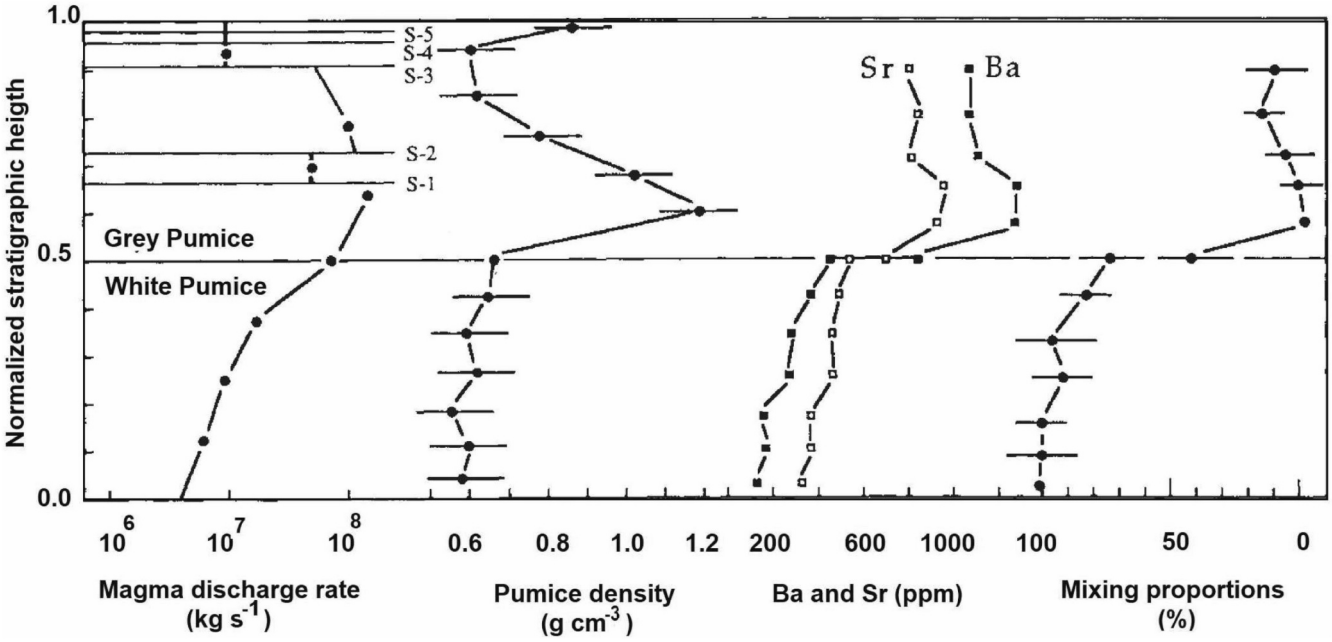

Fig. 13. Variation in magma discharge rate, pumice density, Ba and Sr content of pumice during the Plinian stage of the 79 CE eruption of Vesuvius, shown as a function of normalized stratigraphic height in the pumice fallout deposit. Horizontal lines labelled S-1 to S-5 correspond to the stratigraphic position of intraplinian surge deposits (from Sigurdsson et al., 1990, modified).

non-silicate liquid (chloride-carbonate-sulfate) nucleate and grow around the vapor bubbles (Fig. 9) forming larger fluid pockets (or bubbles). It is possible that, on large scale as well, during *syn*-eruptive cooling of magma, at the same temperature, the same liquid droplets form joining to the vapor bubbles increasing explosiveness of the eruptions, even at open conduit condition. This could be the case of the 79 CE Pompei eruption, which as stated by Sigurdsson et al. (1990) during the first part of the eruption, ejected white pumices with a rate increasing from 5×10^6 to 8×10^7 kg s^{-1}. After seven hours of Plinian activity, the magma composition changed abruptly to grey pumices and, contrary to expectations, the magma discharge rate continued to increase to a peak value of 1.4×10^8 kg s^{-1} generating the first pyroclastic flow and surge (S-1) (Fig. 13). The mechanisms for melt unmixing and kinetics of droplet nucleation and growth have already been reported by James (1975) and by Mazurin and Porai-Koshits (1984).

6. Summary

In this review, various aspects of the SV volcanic system have been highlighted that have not yet been clarified despite the large number of studies carried out so far. The results of previous studies on FI and MI in SV skarn minerals have been reported, together with new data on composite melt inclusions (CMI), as it is believed that the new microthermometric observations can provide a new interpretation for still unresolved issues.

The new finding is the immiscibility between silicate liquids (SLI), with different chemical compositions which could explain the observed stratification in SV shallow magma chamber.

Composite melt inclusions (CMI) found for the first time in SV skarn minerals record at micrometric scale the complete sequence of all phases of magma cooling. At a pressure of 100 MPa, CMI show two types of immiscibility: (1) one between presumably two silicate liquids at about 1060 °C and (2) another between silicate melt and hydrosaline melt at about 700 °C.

Magmatic differentiation by SLI is almost never taken into consideration at a large scale and for this reason all the previous data supporting this hypothesis must be considered. If CMI accurately reproduces on a small scale the sequence of phase separation events in the shallow magma suggests that the magma on cooling at $T < 1060$ °C, unmixes forming two different silicate melts independently evolving to different degrees and over time becoming stratified. Once two melts unmix, they behave as different magmas, with petrological signatures

which can be misinterpreted as magma mixing and/or mingling.

After the caldera formation, during the long repose time, the steady-state magma differentiated by SLI. The less dense magma feeding Plinian eruptions settled on the top, within the "transition zone" (between the magma dominated system and the hydrothermal fluids dominated system) undergoing geochemical changes, as well as isotopic signatures and water contents, and slowly cooling down. Magma feeding interplinian eruptions settled at the bottom of the shallow magma chamber keeping its chemical composition almost constant as shown by the erupted products.

As observed in SMI and CMI, immiscibility between silicate melt and hydrosaline melt instantly occurs at about 700 °C. We hypothesize that, on large scale as well, during syn-eruptive cooling of magma, at the same temperature, droplets of hydrosaline liquid which aggregate and join to vapor bubbles form acting as propellant and increasing explosiveness of the eruptions.

Silicate liquid immiscibility at relatively high-T has the merit of introducing a new scenery and new ideas to improve the present knowledges of volcanic systems with explosive eruptions and caldera formation.

Supplementary data to this article can be found online at https://doi.org/10.1016/j.gexplo.2023.107348.

Declaration of competing interest

The authors declare that they have no known competing financial interests or personal relationships that could have appeared to influence the work reported in this paper.

Data availability

Data will be made available on request.

Acknowledgments

The authors thank Harvey Belkin and Benedetto De Vivo for their support and for reviewing the first draft, Csaba Szabo for his constructive review, an anonymous reviewer for his/her suggestions and Sergio Bravo for samples preparations.

References

Auger, E., Gasparini, P., Virieux, J., Zollo, A., 2001. Seismic evidence of an extended magmatic sill under Mt Vesuvius. Science 294, 1510–1512.

Ayuso, R.A., De Vivo, B., Rolandi, G., Seal II, R.R., Paone, A., 1998. Geochemical and isotopic Nd–Pb–Sr–O variations bearing on the genesis of volcanic rocks from Vesuvius, Italy. In: Spera, F.J., De Vivo, B., Ayuso, R.A., Belkin, H.E. (Eds.), Vesuvius Special Issue. J. Volcanol. Geotherm. Res, 82, pp. 53–78.

Belkin, H.E., De Vivo, B., 1993. Fluid inclusion studies of ejected nodules from plinian eruptions of Mt. Somma-Vesuvius. In: De Vivo, B., Scandone, R., Trigila, R. (Eds.), Vesuvius Special Issue. J. Volcanol. Geoth. Res, 58, pp. 89–100.

Belkin, H.E., De Vivo, B., Roedder, E., Cortini, M., 1985. Fluid inclusion geobarometry from ejected Mt. Somma-Vesuvius nodules. Am. Mineral. 70, 288–303.

Belkin, H.E., De Vivo, B., Lima, A., Torok, K., 1996. Magmatic silicate/saline/sulfur-rich/CO_2 immiscibility and zirconium and rare-earth element enrichment from alkaline magma chamber margins: evidence from Ponza island, Pontine Archipelago, Italy. Eur. J. Mineral. 8 (5), 1401–1420.

Belkin, H.E., De Vivo, B., Torok, K., Webster, J.D., 1998. Pre-eruptive volatile content, melt-inclusion chemistry, and microthermometry of interplinian Vesuvius lavas (pre-A.D. 1631). In: Spera, F.J., De Vivo, B., Ayuso, R.A., Belkin, H.E. (Eds.), Vesuvius Special Issue. J. Volcanol. Geotherm. Res, 82, pp. 79–95.

Belkin, H.E., Horton, 2009. In: Gohn, G.S., Koeberl, C., Miller, K.G., Reimold, W.U. (Eds.), The ICDP-USGS Deep Drilling Project in the Chesapeake Bay Impact Structure: Results from the Eyreville Core Holes, 458. Geological Society of America Special Paper, pp. 447–468. https://doi.org/10.1130/2009.2458(20).

Bernasconi, A., Bruni, P., Gorla, L., Principe, C., Sbrana, A., 1981. Risultati preliminari dell'esplorazine geotermica profonda nell'area vulcanica del Somma-Vesuvio. Rend. Soc. Geol. Ital. 4, 237–240.

Berrino, G., Corrado, G., Riccardi, U., 1998. Sea gravity data in the Gulf of Naples: a contribution to delineate the structural pattern of the Vesuvius area. In: Spera, F.J., De Vivo, B., Ayuso, R.A., Belkin, H.E. (Eds.), Vesuvius Spec Issue J. Volcanol. Geotherm. Res, pp. 82,139–151.

Bertagnini, A., Landi, P., Rosi, M., Vigliargio, A., 1998. The Pomici di Base plinian eruption of Somma-Vesuvius. J. Volcanol. Geotherm. Res. 83, 219–239.

Bodnar, R.J., Cannatelli, C., De Vivo, B., Lima, A., Belkin, H.E., Milia, A., 2007. Quantitative model for magma degassing and ground deformation (bradyseism) at Campi Flegrei, Italy: implications for future eruptions. Geology 35, 791–794. https://doi.org/10.1130/G23653A.1.

Brocchini, D., Principe, C., Castradori, D., Laurenzi, M.A., Gorla, L., 2001. Quaternary evolution of the southern sector of the Campanian Plain and early Somma-Vesuvius activity: insights from the Trecase 1 well. Mineral. Petrol. 73, 67–91.

Buono, G., Pappalardo, L., Harris, C., Edwards, B.R., Petrosino, P., 2020. Magmatic stoping during the caldera-forming Pomici di Base eruption (Somma-Vesuvius, Italy) as a fuel of eruption explosivity. Lithos V. 370–371, 105628. https://doi.org/10.1016/j.lithos.2020.105628.

Cannatelli, C., 2020. Tracing magma evolution at Vesuvius volcano using melt inclusions: a review. In: De Vivo, B., Belkin, H.E., Rolandi, G. (Eds.), Vesuvius, Campi Flegrei and Campanian Volcanism. Elsevier, pp. 121–134. ISBN: 978-0-12-816454-9.

Cannatelli, C., Doherty, A.L., Esposito, R., Lima, A., De Vivo, B., 2016. Understanding a volcano through a droplet: a melt inclusion approach. J. Geochem. Explor. 171, 4–19. https://doi.org/10.1016/j.gexplo.2015.10.003. Special Issue; Ni et al., Eds.

Caricchi, L., Townsend, M., Rivalta, E. Atsuko, N., 2021. The build-up and triggers of volcanic eruptions. Nat. Rev. Earth Environ. 2, 458–476. https://doi.org/10.1038/s43017-021-00174-8.

Cioni, R., 2000. Volatile content and degassing processes in the AD 79 magma chamber at Vesuvius (Italy). Contrib. Mineral. Petrol. 140, 40–54.

Cioni, R., Civetta, L., Marianelli, P., Metrich, N., Santacroce, R., Sbrana, A., 1995. Compositional layering and syn-eruptive mixing of a periodically refilled magma chamber: the A.D. 79 plinian eruption of Vesuvius. J. Petrol. 36, 739–776.

Civetta, L., Santacroce, R., 1992. Steady state magma supply in the last 3400 years of Vesuvius activity. Acta Vulcanol. 2, 147–159.

Civetta, L., Galati, R., Santacroce, R., 1991. Magma mixing and convective compositional layering within the Vesuvius magma chamber. Bull. Volcanol. 53, 287–300.

De Natale, G., Troise, C., Trigila, R., Dolfi, D., Chiarabba, C., 2003. Seismicity and 3D sub-structure at Somma-Vesuvius volcano: evidence for magma quenching. Earth Planet. Sci. Lett. 221, 181–196.

De Natale, G., Troise, C., Pingue, F., Mastrolorenzo, G., Pappalardo, L., 2006. The Somma Vesuvius volcano (Southern Italy): structure, dynamics and hazard evaluation. Earth Sci. Rev. 74, 73–111.

De Vivo, B., Frezzotti, M.L., Mahood, G., 1992. Fluid inclusions in xenoliths yield evidence for fluid evolution in peralkaline granitic bodies at Pantelleria (Italy). J. Volcanol. Geotherm. Res. 52, 295–301.

De Vivo, B., Frezzotti, M.L., Lima, A., 1993. Immiscibility in magmatic differentiation and fluid evolution in granitoid xenoliths at Pantelleria: fluid inclusions evidence. Acta Vulcanol. 3, 195–202.

De Vivo, B., Torok, K., Ayuso, R.A., Lima, A., Lirer, L., 1995. Fluid inclusion evidence for magmatic silicate/saline immiscibility and isotope geochemistry of alkaline xenoliths from Ventotene island (Italy). Geochim. Cosmochim. Acta 59 (14), 2941–2953.

De Vivo, B., Ayuso, R.A., Belkin, H.E., Fedele, L., Lima, A., Rolandi, G., Somma, R., Webster, J.D., 2003. Chemistry, fluid/melt inclusions and isotopic data of lavas, tephra and nodules from ~25 ka to 1944 AD of the Mt Somma-Vesuvius volcanic activity, Mt Somma-Vesuvius. In: Geochemical Archive Dipartimento di Geofisica e Vulcanologia, Università di Napoli Federico II, Open File Report 1–2003, pp. 1–143.

De Vivo, B., Lima, A., Kamenetsky, V.S., Danyushevsky, L.V., 2006. Fluid and melt inclusions in the sub-volcanic environments from volcanic systems: examples from the Neapolitan area and Pontine Islands, Italy. In: Webster, J.D. (Ed.), Melt Inclusions in Plutonic Rocks, Short Course Series V 36. Mineralogical Association of Canada, Montreal, Quebec, Canada. ISBN 0-921294-36-0.

Di Maio, R., Mauriello, P., Patella, D., Petrillo, Z., Piscitelli, S., Siniscalchi, A., 1998. Electric and electromagnetic outline of the 1378 Mt. Somma-Vesuvius structural setting. J. Volcanol. Geotherm. Res. 82, 219–238.

Di Renzo, V., Di Vito, M.A., Arienzo, I., Carandente, A., Civetta, L., D'Antonio, M., Giordano, F., Orsi, G., Tonarini, S., 2007. Magmatic history of Somma-Vesuvius on the basis of new geochemical and isotopic data from a deep borehole (Camaldoli della Torre). J. Petrol. 48, 753–784.

Di Renzo, V., Perullo, C., Arienzo, I., Civetta, L., Petrosino, P., D'Antonio, M., 2022. Geochemical and Sr-isotopic study of clinopyroxenes from Somma-Vesuvius Lavas: inferences for magmatic processes and eruptive behavior. Minerals 12 (9), 1114. https://doi.org/10.3390/min12091114.

Esposito, R., 2021. Chapter 7. A protocol and review of methods to select, analyze and interpret melt inclusions to determine pre-eruptive volatile contents of magmas. In: Lecumberri-Sanchez, P., Steele-MacInnis, M., Kontak, D. (Eds.), Fluid and Melt Inclusions: Applications to Geologic Processes. Mineralogical Association of Canada, London, Ontario, pp. 163–194.

Esposito, R., Klebesz, R., Bartoli, O., Klyukin, Y.I., Moncada, D., Doherty, A.L., Bodnar, R. J., 2012. Application of the Linkam TS1400XY heating stage to melt inclusion studies. Cent. Eur. J. Geosci. 4, 208–218. https://doi.org/10.2478/S13533-011-0054-Y.

Esposito, R., Redi, D., Danyushevsky, L., Gurenko, A., De Vivo, B., Manning, C., et al., 2023. Constraining the volatile evolution of mafic melts at Mt. Somma–Vesuvius, Italy, based on the composition of reheated melt inclusions and their olivine hosts. Eur. J. Mineral. 35 (6), 921–948 [10.5194/ejm-35-921-2023].

Fedele, L., Tarzia, M., Belkin, H.E., De Vivo, B., Lima, A., Lowenstern, J.B., 2006. Magmatic-hydrothermal fluid interaction and mineralization in alkali-syenite nodules from the Breccia Museo pyroclastic deposit, Naples, Italy. In: De Vivo, B. (Ed.), Volcanism in the Campania Plain: Vesuvius, Campi Flegrei and Ignimbrites, Developments in Volcanology, 9. Elsevier, pp. 125–161.

Fedi, M., Florio, G., Rapolla, A., 1998. 2.5D modelling of Somma-Vesuvius structure by aeromagnetic data. J. Volcanol. Geotherm. Res. 82, 239–247.
Fulignati, P., Kamenetsky, V.S., Marianelli, P., Sbrana, A., Mernagh, T.P., 2001. Melt inclusion record of immiscibility between silicate, hydrosaline, and carbonate melts: applications to skarn genesis at Mount Vesuvius. Geology 29, 1043–1046.
Fulignati, P., Kamenetsky, V.S., Marianelli, P., Sbrana, A., 2005. Fluid inclusion evidence of second immiscibility within magmatic fluids (79 AD eruption of Mt. Vesuvius). Period. Miner. 74, 43–54.
Geshi, N., 2020. Volcanological challenges to understanding explosive large-scale eruptions. Earth Planets Space 72, 99. https://doi.org/10.1186/s40623-020-01222-1.
Gilg, H.A., Lima, A., Somma, R., Belkin, H.E., De Vivo, B., Ayuso, R.A., 2001. Isotope geochemistry and fluid inclusion study of skarns from Vesuvius. Mineral. Petrol. 73, 145–176.
Gudmundsson, A., 2020. Volcanotectonics: Understanding the Structure, Deformation and Dynamics of Volcanoes. Cambridge University Press, Cambridge. https://doi.org/10.1017/9781139176217.
Hermes, O.D., Cornell, W.C., 1978. Petrochemical Significance of Xenolithic Nodules Associated With Potash-rich Lavas of Somma-Vesuvius Volcano, NSF Final Technical Report. University of Rhode Island, p. 58.
Hermes, O.D., Cornell, W.C., 1981. Quenched crystal mush and associated magma compositions as indicated by intercumulus glasses from Mt. Vesuvius, Italy. J. Volcanol. Geotherm. Res. 9, 133–149.
Hermes, O.D., Cornell, W.C., 1983. The significance of mafic nodules in the ultra-potassic rocks from central Italy-reply. J. Volcanol. Geotherm. Res. 16, 166–172.
Holness, M., Nielsen, T., Tegner, C., 2017. The Skaergaard intrusion of East Greenland: paradigms, problems and new perspectives. Elements V13. https://doi.org/10.2138/gselements.13.6.391.
James, P.F., 1975. Liquid phase separation in glass-forming systems. J. Mater. Sci. 10, 1802–1825.
Kamenetsky, V.S., 2006. Melt inclusion record of magmatic immiscibility in crustal and mantle magmas. Mineralogical Association of Canada Short Course 36, Montreal, Quebec, pp. 81–98.
Kamenetsky, V.S., De Vivo, B., Naumov, V.B., Kamenetsky, M.B., Mernagh, T.P., Van Achterbergh, E., Ryan, C.G., Davidson, P., 2003. Magmatic inclusions in the search for natural silicate-salt melt immiscibility: methodology and examples. In: De Vivo, B., Bodnar, R.J. (Eds.), Developpements in Volcanology, 5, Melt Inclusions in Volcanic System:Mthods, Applications and Problems. Elsevier, Amsterdam, pp. 65–82.
Kelemework, Y., Milano, M., La Manna, M., de Alteriis, G., M. Iorio, M., Fedi, M., 2021. Crustal structure in the Campanian region (Southern Apennines, Italy) from potential field modelling. Sci. Report. 11, 14510. https://doi.org/10.1038/s41598-021-93945-8.
Klébesz, R., Bodnar, R., De Vivo, B., Török, K., Lima, A., Petrosino, P., 2012. Composition and origin of nodules from the ~20 ka Pomici di Base (PB)-Sarno eruption of Mt. Somma-Vesuvius, Italy. Centr. Eur. J. Geosci. 4, 324–337.
Klébesz, R., Esposito, R., De Vivo, B., Bodnar, R.J., 2015. Further constraints on the origin of nodules from the Sarno (Pomici di Base) eruption of Mt. Somma-Vesuvius (Italy) based on reheated silicate-melt inclusions and clinopyroxene composition. Am. Mineral. 100, 760–773. https://doi.org/10.2138/am-2015-4958.
Landi, P., Bertagnini, A., Rosi, M., 1999. Chemical zoning and crystallization mechanisms in the magma chamber of the Pomici di Base plinian eruption of Somma-Vesuvius (Italy). Contrib. Mineral. Petrol. 135, 179–197.
Lentz, D., 1999. Carbonatite genesis: a reexamination of the role of intrusion-related pneumatholytic skarn processes in limestone melting. Geology 27, 335–338.
Lentz, D., 2017. Syntectic reactions involving limestones and limestone-derived carbonatitic melts in the generation of some peralkalic magmas: reflections on Reginald Daly's insights 100 years later. In: American Geophysical Union, Fall Meeting 2017, Abstract #V53A-03.
Lima, A., Belkin, H.E., Torok, K., 1999. Understanding Vesuvius magmatic processes: evidence from primitive silicate-melt inclusions in medieval scoria clinopyroxenes (Terzigno Formation). Mineral. Petrol. 65, 185–206.
Lima, A., Danyushevsky, L.V., De Vivo, B., Fedele, L., Bodnar, R.J., 2003. A model for the evolution of the Mt. Somma-Vesuvius magmatic system based on fluid and melt inclusion investigations. In: De Vivo, B. (Ed.), Melt Inclusions in Volcanic Systems: Methods, Applications and Problems, Developments in Volcanology Series, 5. Elsevier - Amsterdam, pp. 227–249. ISBN 0-444-51151-2.
Lima, A., De Vivo, B., Fedele, L., Sintoni, M.F., 2006. Influence of hydrothermal processes on geochemical variations between 79 AD and 1944 AD Vesuvius eruptions. In: De Vivo, B. (Ed.), Volcanism in the Campania Plain: Vesuvius, Campi Flegrei and Ignimbrites, Developments in Volcanology, 9. Elsevier, pp. 235–247. ISBN 0 444 52175 5.
Lima, A., De Vivo, B., Fedele, L., Sintoni, M.F., Milia, A., 2007. Geochemical variations between the 79 AD and 1944 AD Mt. Somma-Vesuvius volcanic products: constraints on the evolution of the hydrothermal system based on fluid and melt inclusions. Chem. Geol. 237, 401–417. https://doi.org/10.1016/j.chemgeo.2006.07.011.
Lima, A., De Vivo, B., Spera, F.J., Bodnar, R.J., Milia, A., Nunziata, C., Belkin, H.E., Cannatelli, C., 2009. Thermodynamic model for the uplift and deflation episodes (bradyseism) associated with magmatic-hydrothermal activity at the Campi Flegrei active volcanic center (Italy). Earth Sci. Rev. 97, 44–58. https://doi.org/10.1016/j.earscirev.2009.10.001.
Lima, A., Bodnar, R.J., De Vivo, B., Spera, F.J., Belkin, H.E., 2021. Interpretation of recent unrest events (bradyseism) at Campi Flegrei, Napoli (Italy): comparison of models based on cyclical hydrothermal events versus shallow magmatic intrusive events. Geofluids, 2000255. https://doi.org/10.1155/2021/2000255.
Linde, N., Ricci, T., Baron, L., Shakas, A., Berrino, G., 2017. The 3-D structure of the Somma-Vesuvius volcanic complex (Italy) inferred from new and historic gravimetric data. Sci. Report. 7, 8434. https://doi.org/10.1038/s41598-017-07496-y.
Lino, L.M., Carvalho, P.R., Vlach, S.R.F., Quiroz-Valle, F.R., 2023. Evidence for silicate liquid immiscibility in recharging, alkali-rich tholeiitic systems: the role of unmixing in the petrogenesis of intermediate, layered plutonic bodies and bimodal volcanic suites. LITHOS 450–451, 107193. https://doi.org/10.1016/j.lithos.2023.107193.
Lowenstern, J.B., 1993. Immiscibility between silicate melt, vapor and hydrosaline melt (~70-80 wt.% NaCl) in peralkaline rhyolites from Pantelleria, Italy. EOS 74, 670.
Lowenstern, J.B., 1994. Chlorine, fluid immiscibility, and degassing in peralkaline magmas from Pantelleria, Italy. Am. Mineral. 79, 353–369.
Mazurin, O.V., Porai-Koshits, E.A., 1984. Phase Separation in Glass. North-Holland, Amsterdam, Oxford, New York, Tokyo. https://doi.org/10.1002/bbpc.19850891127.
Melluso, L., Scarpati, C., Zanetti, A., Sparice, D., de' Gennaro, R., 2022. The petrogenesis of chemically zoned, phonolitic, Plinian and sub-Plinian eruptions of Somma-Vesuvius, Italy: role of accessory phase removal, independently filled magma reservoirs with time, and transition from slightly to highly silica undersaturated magmatic series in an ultrapotassic stratovolcano. Lithos 430–431, 106854. https://doi.org/10.1016/j.lithos.2022.106854.
Milia, A., Torrente, M.M., 2020. Space-time evolution of an active volcanic field in an extensional region: the example of the Campania margin (eastern Tyrrhenian Sea). In: De Vivo, B., Belkin, H.E., Rolandi, G. (Eds.), Vesuvius, Campi Flegrei and Campanian Volcanism. Elsevier, pp. 297–320. ISBN: 978-0-12-816454-9.
Milia, A., Torrente, M.M., Russo, M., Zuppetta, A., 2003. Tectonics and crustal structure of the Campania continental margin: relationships with volcanism. Mineral. Petrol. 79, 33–47.
Nunziata, C., Costanzo, M.R., Panza, G.F., 2020. Lithosphere structural model of the Campania Plain. In: De Vivo, B., Belkin, H.E., Rolandi, G. (Eds.), Vesuvius, Campi Flegrei and Campanian Volcanism. Elsevier, pp. 57–75. ISBN: 978-0-12-816454-9.
Pappalardo, L., Buono, G., 2021. Insights into processes and timescales of magma storage and ascent from textural and geochemical investigations: case studies from high-risk neapolitan volcanoes (Italy). In: Masotta, M., Beier, C., Mollo, S. (Eds.), Crustal Magmatic System Evolution: Anatomy, Architecture, and Physico-chemical Processes, 2021. John Wiley & Sons, Hoboken, NJ, USA, pp. 213–235.
Peccerillo, A., 2003. Plio-Quaternary magmatism in Italy. Episodes 26, 222–226.
Peccerillo, A., 2020. Campania volcanoes: petrology, geochemistry, and geodynamic significance. In: De Vivo, B., Belkin, H.E., Rolandi, G. (Eds.), Vesuvius, Campi Flegrei and Campanian Volcanism. Elsevier, pp. 79–113. ISBN: 978-0-12-816454-9.
Philpotts, A.R., 1979. Silicate liquid immiscibility in tholeiitic basalts. J. Petrol. 20, 99–118.
Philpotts, A.R., 1982. Compositions of immiscible liquids in volcanic rocks. Contr. Mineral. and Petrol. 80, 201–218. https://doi.org/10.1007/BF00371350.
Pierantoni, P.P., Penza, G., Macchiavelli, C., Schettino, A., Turco, E., 2020. Kinematics of the Tyrrhenian-Apennine system and implications for the origin of the Campanian magmatism. In: De Vivo, B., Belkin, H.E., Rolandi, G. (Eds.), Vesuvius, Campi Flegrei and Campanian Volcanism. Elsevier, pp. 79–113. ISBN: 978-0-12-816454-9.
Piochi, M., Ayuso, R.A., De Vivo, B., Somma, R., 2006. Crustal contamination and crystal entrapment during polybaric magma evolution at Mt. Somma-Vesuvius volcano, Italy: geochemical and Sr isotope evidence. Lithos 86, 303–329.
Roedder, E., 1979. Origin and significance of magmatic inclusions. Bull. Mineral. 102, 487–510.
Rolandi, G., Maraffi, S., Petrosino, P., Lirer, L., 1993. The Ottaviano eruption of Somma-Vesuvius (3760y BP): a magmatic alternating fall and flow-forming eruption. In: De Vivo, B., Scandone, R., Trigila, R. (Eds.), Vesuvius Spec Issue. J Volcanol Geotherm Res, 58, pp. 43–65.
Rolandi, G., Petrosino, P., McGeehin, J., 1998. The interplinian activity at Somma-Vesuvius in the last 3500 years. J. Volcanol. Geotherm. Res. 82, 19–52.
Rolandi, G., Munno, R., Postiglione, I., 2004. The A.D. 472 eruption of the Somma volcano. J. Volcanol. Geotherm. Res. 129, 291–319.
Rose-Koga, E., Bouvier, A.-S., Gaetani, G., Wallace, P., Allison, C., Andrys, J., de la Torre, C.A., Barth, A., Bodnar, R., Gartner, A.B., 2021. Silicate melt inclusions in the new millennium: a review of recommended practices for preparation, analysis, and data presentation. Chem. Geol. 570, 120145.
Santacroce, R. (Ed.), 1987. Somma-Vesuvius, 114. CNR Quad. Ric. Sci, pp. 1–255.
Santacroce, R., Cioni, R., Marianelli, P., Sbrana, A., Sulpizio, R., Zanchetta, G., Donahue, D.J., Joron, J.L., 2008. Age and whole rock-glass compositions of proximal pyroclastics from the major explosive eruptions of Somma-Vesuvius: a review as a tool for distal tephrostratigraphy. J. Volcanol. Geotherm. Res. 177, 1–18.
Sbrana, A., Cioni, R., Marianelli, P., Sulpizio, R., Andronico, D., Pasquini, G., 2020. Volcanic evolution of the Somma-Vesuvius Complex (Italy). J. Maps 16 (2), 137–147. https://doi.org/10.1080/17445647.2019.1706653.
Sigurdsson, H., Cornell, W., Carey, S., 1990. Influence of magma withdrawal on compositional gradients during the AD 79 Vesuvius eruption. Nature 345, 519–521.
Turner, F.J., 1981. Metamorphic Petrology Mineralogical, Field and Tectonic Aspects. McGraw-Hill, New York.
Veksler, I.V., 2004. Liquid immiscibility and its role at the magmatic–hydrothermal transition: a summary of experimental studies. Chem. Geol. 210, 7–31. https://doi.org/10.1016/j.chemgeo.2004.06.002.
Veksler, I.V., Charlier, B., 2015. Silicate liquid immiscibility in layered intrusion. In: Charlier, B., et al. (Eds.), Layered Intrusion. Springer Geology. Doi 10.1007 978. 94-017 96-52 1_5.
Veksler, I.V., Dorfman, A.M., Borisov, A.A., Wirth, R., Dingwell, D.B., 2007. Liquid immiscibility and the evolution of basaltic magma. J. Petrol. 48, 2187–2210.

Wallace, P.J., Plank, T., Bodnar, R.J., Gaetani, G.A., Shea, T., 2021. Olivine-hosted melt inclusions: a microscopic perspective on a complex magmatic world. Annu. Rev. Earth Planet. Sci. 49, 465–494.

Zollo, A., Gasparini, P., Virieux, J., Le Meur, H., De Natale, D., Biella, G., Boschi, E., Capuano, P., De Franco, R., Dell'Aversana, P., De Matteis, R., Guerra, I., Iannaccone, G., Mirabile, L., Vilardo, G., 1996. Seismic evidence for a low-velocity zone in the upper crust beneath Mount Vesuvius. Science 274, 592–594.

Zollo, A., Gasparini, P., Virieux, J., Biella, G., Boschi, E., Capuano, P., de Franco, R., dell'Aversana, P., de Matteis, R., De Natale, G., Iannaccone, G., Guerra, I., Le Meur, H., Mirabile, L., 1998. An image of Mt. Vesuvius obtained by 2D seismic tomography. J. Volcanol. Geotherm. Res. 82, 161–174.